

# Phase Contrast Computed Tomography Using Continuous THz Source

M.Suga<sup>1</sup>, Y.Sasaki<sup>2</sup>, T. Sasahara<sup>1</sup>, T.Yuasa<sup>1</sup>, C.Otani<sup>2</sup>

<sup>1</sup> Graduate School of Science and Engineering, Yamagata University, Yamagata, Japan

<sup>2</sup> Terahertz Sensing and Imaging Team, RIKEN, Miyagi, Japan

E-mail: yuasa@yz.yamagata-u.ac.jp

**Abstract** – We propose a novel computed tomography (CT) imaging method based on phase-contrast using a continuous wave (CW) THz source with a frequency of 0.54 THz. The system acquires phase-shift by phase modulation technique using Mach-Zehnder interferometer at each data point, and collects projections of the phase-shift from multiple directions over 360 degrees to finally reconstruct a spatial distribution of refractive index. We construct a preliminary system for proof of the concept, and perform an imaging experiment using a polystyrene foam phantom. It was shown that the THz-CT produces an artifact-free and quantitative reconstruction at a spatial resolution of a few mm.

**Keywords** – phase contrast, computed tomography, Mach-Zehnder interferometer, refractive index

## I. INTRODUCTION

The terahertz (THz) wave is an electromagnetic wave with a frequency that lies between radio and infrared frequencies. The frequency of the THz wave ranges from 0.1 to 10 THz, corresponding to a wavelength of 3 mm – 30  $\mu\text{m}$ . The recent development of THz optical devices has accelerated research to THz imaging [1-7]. A variety of imaging methods have been proposed to take advantage of the characteristics of THz waves. The high transmissivity of THz waves for some materials enables tomographic imaging analogous to X-ray computed tomography (CT) [8].

However, as many of conventional THz-CTs form contrast based on attenuation of the incident beam intensity in a way similar to an x-ray CT, remarkable artifacts, i.e., cupping artifacts, appear at the boundary of a reconstructed object because of the unintended intensity dissipation at the boundaries caused by refraction and scattering due to the mismatch of refractive index [9, 10], leading to impaired quantitative observations. In contrast, the phase-shift is not influenced by the intensity dissipation at the boundary, so artifact-free reconstruction is expected as long as the transmitted wave can be detected.

In this study, we propose a THz-CT method based on phase contrast with significantly reduced artifacts. The THz-CT is based on the first generation type of CT, which acquires a set of projections by translation and rotational scans using a thin beam. At each data-point, the projection data of phase-shift is estimated by phase

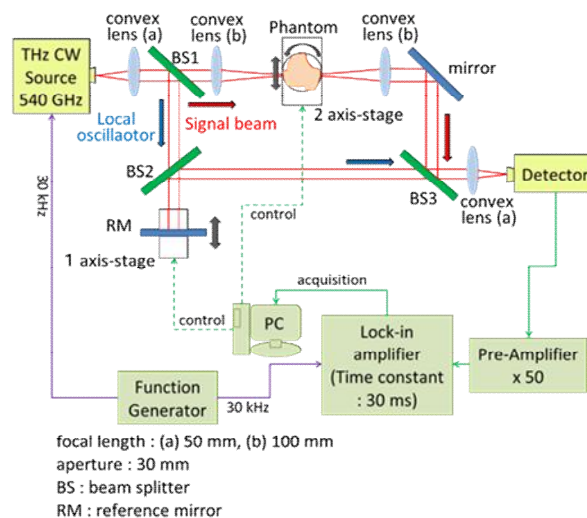


Fig. 1. Phase-shift THz-CT system based on Mach-Zehnder interferometer.

modulation technique using Mach-Zehnder interferometer with a continuous wave (CW) source. From the projections of phase-shift we reconstruct a spatial distribution of refractive index in a cross section of interest. We constructed a preliminary system to prove the concept, and performed an imaging experiment using a polystyrene foam phantom to show the effectiveness of the proposed method.

## II. EXPERIMENTAL SETUP AND IMAGING PRINCIPLE

**Fig. 1** shows a schematic of THz-CT imaging system based on Mach-Zehnder interferometer. A frequency-multiplier CW source with a frequency of 540 GHz and a wavelength of 550  $\mu\text{m}$  (Virginia Diodes, Inc.) is used as a light source. The amplitude of the THz wave from the source is modulated at 30 kHz with a rectangular waveform generated by a function generator. The THz wave, collimated with convex lens and concave mirrors to a thin parallel beam with a beam diameter of approximately 2.5 mm, is split into the signal and the local oscillator beam at the beam splitter BS1. The signal beam impinges on a sample, which is mounted on positioning devices to translate and rotate, is subject to a variety of optical phenomena, e.g., refraction, reflection, attenuation, and scattering, according to a distribution of

refractive-index in the sample. The signal beam passing through the sample and preserving the propagation direction is mixed with the local oscillator beam, whose path length is adjusted with the reference mirror RM, at the beam splitter BS3. The mixed beam is detected by a Schottky-barrier diode detector. The detected signal was fed into a preamplifier (with a gain of 5000) followed by a lock-in amplifier (time constant: 30 ms), then fed to a personal computer through a data acquisition card.

Below, we quantitatively consider how the phase-shift is estimated from the measured data. First, we consider the case that there is no sample. We denote by  $E_S = A_S \exp(ikz_S)$  the signal wave, where  $k = 2\pi/\lambda$ , and  $A_S$  and  $z_S$  are the amplitude and the path length of the signal arm, respectively. On the other hand, we denote by  $E_L = A_L \exp(ikz_L)$  the local oscillator wave, where  $A_L$  and  $z_L$  are the amplitude and the path length of the local oscillator arm, respectively. The output signal is proportional to the value given as

$$|E_S + E_L|^2 = A_S^2 + A_L^2 + 2A_S A_L \cos k(z_S - z_L) .$$

Next, we consider that there is a sample. Here, after introducing the  $z$ -axis along the signal beam passing through the sample, we set  $z = 0$  and  $z = t$  at the points on which the signal beam is incident and from which it outgoes, respectively. In this case, the signal wave on the detectable surface is given as

$$E_S = A_S \exp\{ik(z_S - t)\} \exp\left\{ik \int_0^t (n + i\kappa) dz\right\} ,$$

where  $n + i\kappa$  is a complex refractive index being a function of  $z$ . Rearranging, we obtain

$$E_S = A_S \exp\left\{-\int_0^t \mu dz\right\} \exp\left\{ik\left(z_S - t + \int_0^t n dz\right)\right\} ,$$

where  $\mu = k\kappa$ . Therefore, the output signal is given as

$$\begin{aligned} I(z_S - z_L) &= |E_S + E_L|^2 \\ &= A_S^2 \exp\left\{-2 \int_0^t \mu dz\right\} + A_L^2 + \\ &\quad 2A_S A_L \exp\left\{-\int_0^t \mu dz\right\} \cos\left\{k\left(\int_0^t n dz - t + z_S - z_L\right)\right\} \end{aligned}$$

Rewriting simply,

$$I(z_S - z_L) = I_D + I_A \cos\{k(\phi + z_S - z_L)\} , \quad (1)$$

where

$$I_D = A_S^2 \exp\left\{-2 \int_0^t \mu dz\right\} + A_L^2 , \quad (2)$$

$$I_A = 2A_S A_L \exp\left\{-\int_0^t \mu dz\right\} , \quad \text{and} \quad (3)$$

$$\phi = \int_0^t (n-1) dz . \quad (4)$$

Then, we estimate a phase-shift  $\phi$  from multiple data obtained while adjusting  $z_L$ . That is, we acquire four data under the conditions  $z_S - z_L = 0, \lambda/4, \lambda/2, 3\lambda/4$  as follows:

$$I(0) = I_D + I_A \cos\{k\phi\} ,$$

$$I(\lambda/4) = I_D - I_A \sin\{k\phi\} ,$$

$$I(\lambda/2) = I_D - I_A \cos\{k\phi\} , \quad \text{and}$$

$$I(3\lambda/4) = I_D + I_A \sin\{k\phi\} .$$

From the above four equations, we can estimate the phase-contrast

$$\phi = \frac{1}{k} \tan^{-1} \frac{I(3\lambda/4) - I(\lambda/4)}{I(0) - I(\lambda/2)} . \quad (5)$$

On the other hand, assuming that the refractive index  $n$  is a unity in air,  $n-1$  is zero in the region outside the sample. Thus,

$$\int_{-\infty}^{\infty} (n-1) dz = \int_0^t (n-1) dz = \phi .$$

This means that the estimated phase-shift is equal to the line integral of  $n-1$  along the signal beam propagation, that is, the projection data of  $n-1$ . Therefore, by collecting the measurements while translating and rotating the sample according to the data-acquisition scheme in the first generation type of CT, we can prepare a set of projections. Using the filtered back projection (FBP) method, we can reconstruct the cross-section from the projections. Noting that the reconstructed image is a spatial distribution of  $n-1$ , we can easily know the refractive-index distribution from the reconstructed image.

On the other hand, we pay attention to Eq. (3). The value is proportional to  $\exp\left\{-\int_0^t \mu dz\right\}$ . Similarly to the

above discussion, assuming that absorption term  $\kappa$  is zero in the region outside the sample, we obtain

$$\exp\left\{-\int_{-\infty}^{\infty} \mu dz\right\} = \exp\left\{-\int_0^t \mu dz\right\} .$$

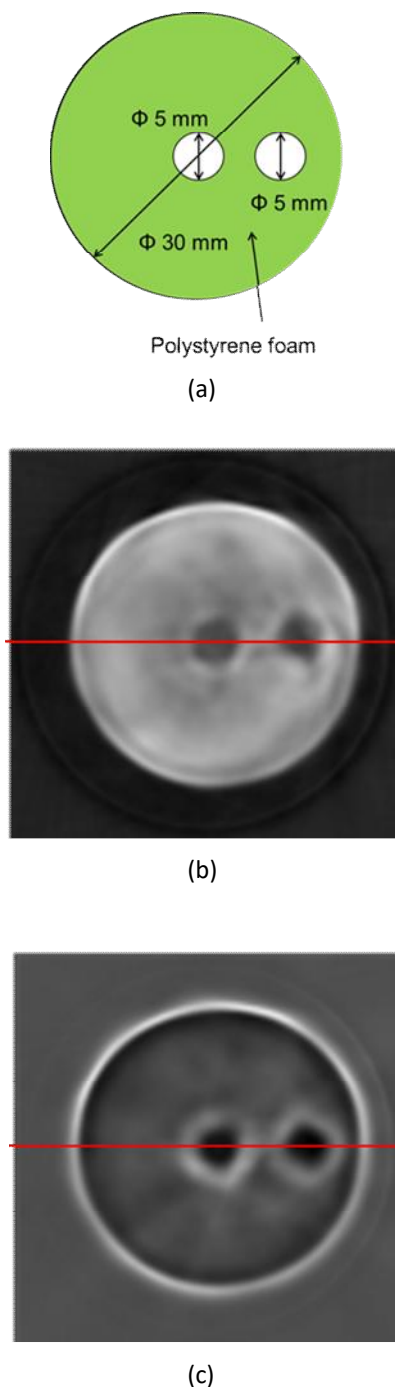


Fig. 2. (a) Schematic of polystyrene foam phantom, (b) THz-CT image based on phase-contrast, (c) THz-CT image based on attenuation-contrast

This is the line integral of absorption coefficient. Therefore, we can obtain the projections of absorption coefficient from the measured data as well at the same time. Of course, we cannot obtain a high-quality reconstructed image, since the absorption projections are contaminated with unexpected reflection, refraction, and scattering at the boundaries with the mismatch of refractive index.

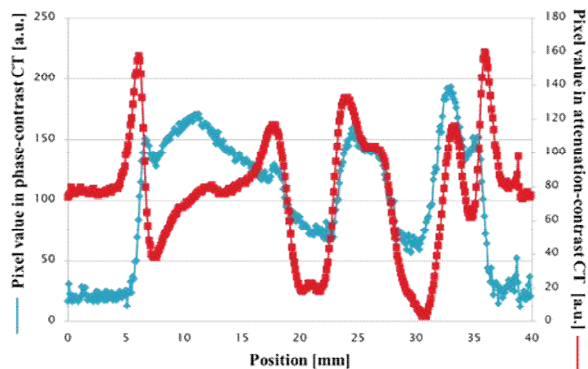


Fig. 3. Profiles of the both images on the red lines indicated in Figs. 2 (b) and (c)

### III. EXPERIMENTAL RESULT

In order to validate the imaging characteristics of the system, we imaged a polystyrene foam sphere of 30 mm in diameter having two channels of 5 mm in diameter (Fig. 2(a)). The sample was fixed on a translation and rotation stages so that the channels were perpendicular to the incident beam. After completing a series of 0.1-mm step translational scanning procedures, the sample was rotated at 1-degree rotational step. A series of data acquisitions were performed over 360 degrees, resulting in 360 projection data. Then, since the estimated phase-shift was wrapped, we applied an unwrap procedure to the projection data. Finally, we reconstructed the cross-section from the unwrapped projections using the filtered backprojection method with a Shepp-Logan filter. Fig. 2 (b) shows a phase-contrast THz-CT image of the phantom at the level where the diameter of cross-section is maximal, which was reconstructed from the projections based on Eq. (5). Fig. 2 (c) shows an attenuation-contrast THz-CT image of the phantom at the same level, which was reconstructed from the projections based on Eq. (3). In the both reconstructed images, the pixel values were normalized in 8-bit gradation. Fig. 3 compares profiles of the both images on the red lines indicated in Figs. 2 (b) and (c), where the vertical and horizontal lines are the pixel value and the position, respectively. The blue and red curves correspond to profiles of phase- and attenuation-contrast CT images, respectively. In the attenuation-contrast CT, remarkable artifacts at the boundary between air and polystyrene foam regions are observed. In addition, the pixel value in some regions is much lower than that of air region, although that of air region is zero. The facts show that the attenuation-contrast CT cannot offer not only artifact-free reconstruction but also quantitative measurement. On the other hand, in the phase-contrast CT image, remarkable artifacts are not observed.

As described in Section 2, the pixel value in the

reconstructed phase-contrast CT image represents the refractive index. Using Eq. (5), we recalculated all the pixel values of **Fig. 2 (b)**. **Fig. 3** shows the profile of refractive index on the red line indicated in **Figs. 2 (b)** and **(c)**. The estimated refractive index in polystyrene foam regions ranges from 1.02 to 1.035, and the average is 1.025 ( $\pm 0.003$ ). In reference [11], it was reported that the refractive index of polystyrene foam ranges from 1.016 to 1.022. The values are similar to our estimated average value.

Although it is reasonable that the estimated refractive indices in air regions outside the sample are almost zero, those in the channel regions take finite values. This will be because the diameter of channels is relatively large compared with the diameter of beam cross-section. If the beam diameter is sufficiently less than the channel diameter, the nonconformity will be dissolved.

#### IV. CONCLUSION

We proposed a novel THz-CT imaging method based on phase-contrast. We constructed a preliminary system for proof of the concept. The system acquires the projections of phase-contrast using a phase modulation technique with Mach-Zehnder interferometer, and reconstructs a distribution of refractive index from the measured projections. The experimental using a physical phantom showed the effectiveness in that the artifacts-free and quantitative reconstruction was feasible.

In the future, we will improve the imaging performance such as spatial resolution, and measurement time, by optimizing the system.

#### REFERENCES

- [1] B. B. Hu, and M. C. Nuss, *Opt. Lett.*, vol.20, no.16, pp.1716-1718 (1995).
- [2] Woodward, R. M., V. P. Wallace, D. D. Arnone, E. H. Linfield, and M. Pepper, *J. Biol. Phys.* 29, 257-261 (2003).
- [3] R. Wilk, F. Breinfeld, M. Mikulics, and M. Koch, *Appl. Opt.* 47, 3023-3026 (2008).
- [4] T. Yasuda, T. Iwata, T. Araki, and T. Yasui, *Appl. Opt.* 46, 7518-7526 (2007).
- [5] T. Kiwa, J. Kondo, S. Oka, I. Kawayama, H. Yamada, M. Tonouchi, and K. Tsukada, *Appl. Opt.* 47, 3324-3327 (2008).
- [6] S. R. Murrill, E. L. Jacobs, S. K. Moyer, C. E. Halford, S. T. Griffin, F. C. De Lucia, D. T. Petkie, and C. C. Franck, *Appl. Opt.* 47, 1286-1297 (2008).
- [7] Y. Kawada, T. Yasuda, H. Takahashi, and S.-I. Aoshima, *Opt. Lett.* 33, 180-182 (2008).
- [8] C. Kak and M. Slaney, "Principles of Computerized Tomographic Imaging," New York: *IEEE Press*, (1987).
- [9] B. Ferguson, S. Wang, D. Gray, D. Abbot, and X. C. Zhang, *Opt. Lett.* 27, 1312-1314 (2002).
- [10] B. Recur, A. Younus, S. Salort, P. Mounaix, B. Chassagne, P. Desbarats, J-P. Caumes, and E. Abraham1, *Opt. Express* 19, 5105-5117 (2011).
- [11] G. Zhao, M. Mors, T. Wenckebach, and P. C. M. Planken, *J. Opt. Soc. Am. B* 19, 1476-1479 (2002).